

SPECTRUM SENSING AND SHARING FOR COGNITIVE RADAR SYSTEMS*

Pietro Stinco¹, Maria S. Greco¹, Fulvio Gini¹, and Braham Himed²

¹ Dipartimento di Ingegneria dell'Informazione, University of Pisa, via G. Caruso 16, 56122 Pisa, Italy

² RF Technology Branch, Air Force Research Lab (AFRL/RYMD), WPAFB, OH 45433, USA

ABSTRACT

This paper deals with the problem of Spectrum Sensing and Spectrum Sharing for Cognitive Radar operating in spectrally dense environments. Spectrum sensing and spectrum sharing are the two main functions that allow a cognitive radar to measure, sense, learn, and be aware of the parameters related to the radio channel characteristics. This paper focuses on the role of Compressed Sensing (CS) in Spectrum Sensing and on the problem of channel parameter estimation for Spectrum Sharing. This paper shows how CS can allow a significant reduction in acquisition time reducing the cost for high-resolution analog-to-digital converters with large dynamic range, and high speed signal processors. We derive an algorithm for estimating the channel parameters that characterize the behaviour of the primary users and a spectrum sharing method that exploits these estimates to minimize the interference between the radar and the primary user. The proposed method optimizes the performance of the radar and, at the same time, limits the interference received by the other users.

Keywords - *Cognitive Radar, Spectrum Sensing, Spectrum Sharing, Compressed Sensing, Channel Modeling, Channel Parameters Estimation.*

* This work has been funded by EOARD grant FA8655-13-1-3011 on "Waveform Diversity and Frequency Sharing Techniques for Cognitive Radar Systems".

1. Introduction

Radar technology has been evolving towards higher resolution, high-precision detection instruments with an ever-increasing list of functionalities. One of the areas that have very good potential of combining the benefits of these developments is multifunctional radar systems. These systems join inside the same system, and simultaneously, multiple functions such as surveillance, tracking, confirmation of false alarm, back-scanning, clutter and interference estimation, which are traditionally performed by dedicated individual radars [1]-[2].

For these reasons, multifunctional radar systems should be able to work with wider frequency bands than traditional radar systems. Clearly, this is in contrast with the growth of activities in the area of civil communications, the emergence of new technologies and new services that involve a strong demand for spectrum allocation inducing a very strong pressure upon the frequency channels currently allocated to radars.

Some portions of the radar bands have been recently allocated to communication services. For instance, the International Telecommunication Union (ITU) decided to allocate the spectrum between 5150 and 5350 MHz and between 5470 and 5725 MHz on a co-primary basis to wireless access systems including RLANs (Radio Local Area Networks) [3]-[4]. In the United States, the National Telecommunications and Information Administration (NTIA) has recently devoted efforts on identifying frequency bands that could be made available for wireless broadband service provisioning. A total of 115 MHz of additional spectrum (1695-1710 MHz and 3550-3650 MHz bands) has been identified for wireless broadband implementation [5].

A recent work [6] focused on the primary-secondary sharing between a radar system and indoor system providing broadband services, considering an Air Traffic Control (ATC) radar operating in the 2.7-2.9 GHz band and a Surveillance Radar in the 16.7-17.3 GHz. The case study analysed in this work is an L-band radar that shares the same frequency band with a JTDIS (Joint Tactical Information Distribution System) radio system, supposed to be the primary user of the channel. The JTIDS is a radio system for exchanging tactical information between aircraft and ground stations or ships and between aircraft. The JTDIS radio system operates in the frequency band 969-1206 MHz, subdivided into sub-channels used for frequency hopping.

From the above examples, it is clear that the availability of frequency spectrum for multifunction radar systems has been severely compromised and the available frequency bands are continuously diminished.

This unique issue of spectrum crowding and steadily increasing radar requirements cannot be addressed by traditional modes of operation. Future systems require the ability to anticipate the behaviour of radiators in the operational environment. This in turn leads to the need for critical and new methodologies based upon cognition as an enabling technology [7]-[12].

The cognitive methodology to reduce mutual interference between the radar and the other radiating elements is based on two main concepts: Spectrum Sensing and Spectrum Sharing. Spectrum Sensing has the goal to recognize the frequencies used by other systems using the same spectrum in real time, while Spectrum Sharing has the goal to limit interference from the radar to other services and vice-versa.

Through these functions, a cognitive radar can obtain necessary observations about the radio frequency channel, such as the presence of other users and the appearance of spectrum opportunities, i.e. spectrum holes where it is possible to transmit without interfering with other users of the channel. After using this information, a cognitive radar is able to adapt its transmit and receive parameters, such as the transmission power and the operating frequency, in order to achieve efficient spectrum utilization.

In cognitive radio terminology, primary users is defined as the users who have higher priority or legacy rights on the usage of a specific part of the spectrum. On the other hand, secondary users, which have lower priority, exploit this spectrum in such a way that they do not cause interference to primary users.

Therefore, secondary users need to have cognitive radio capabilities, such as sensing the spectrum reliably to check whether a primary user is using it and to change the radio parameters to exploit the unused part of the spectrum.

In this work, we analyse the problem of a wideband radar system that shares the same frequency band with a communication system, the frequency band of the communication system is divided into several frequency channels used for dynamic spectrum access. The radar system is the secondary user while the communication system is the primary user of the channel.

As an illustrative example, Figure 1 shows the spectrum opportunities in the frequency channels. As apparent, the available spectrum is divided into narrow chunks of bands. Spectrum opportunity in this dimension means that not all the bands are used

simultaneously at the same time; therefore, some bands might be available for opportunistic usage. To this end, a cognitive radar should detect the spectrum opportunities, selecting the best frequency channels and vacating the frequency when a primary user appears.

In this paper, we focus on two important topics, the use of CS for Spectrum Sensing and the problem of channel parameter estimation for Spectrum Sharing application. In particular, we analyse the use of CS, focusing on how this emerging technology can represent a helpful tool to solve some important problems related to the hardware requirement for the design of a responsive spectrum sensing system, which is able to react to the changes of the operating frequency channel quickly. As a matter of fact, to have high spectrum efficiency and high sensing accuracy, a cognitive radar has to perform real-time wideband monitoring of the licensed spectrum, using a dual-radio architecture [13]-[14], where one chain is dedicated to radar operations while the other chain is dedicated to spectrum sensing. The drawback of such approach is the hardware cost, as the related systems requires high sampling rate and high resolution Analog-to-Digital Converters (ADCs) with large dynamic range, plus the use of high speed signal processors. Moreover, when the required time used to estimate the spectrum occupancy is very short and the monitored frequency band is wide, the current generation ADCs are even unable to collect the required samples at the Nyquist-rate. A signal processing technique that can solve this problem is based on the use of Compressed Sensing.

Recent results on CS state that it is possible to reconstruct a sparse signal from random projections of the sensor data (see e.g. [15]-[17]). The number of random projections can be very small, in proportion to the number of the channels occupied by the other users. Under the hypothesis that the frequency spectrum of the other users is sparse, CS can be profitably used to solve the hardware constraints by reducing the sampling rate and decreasing the computational complexity.

The second problem considered in this paper is the estimation of the channel parameters that describe the behaviour of the primary users of the channels and how to exploit these estimates to minimize the interference between the radar and the communication system.

Analysing the behaviour of the primary users and exploiting the time history of the channel occupancy, the cognitive radar system can evaluate the probability to have a spectrum opportunity, i.e. the probability that the monitored frequency channel is free at the time of transmitting. Evaluating this probability, a cognitive radar can decide

whether it is possible or not to transmit in the monitored frequency channel at the beginning of each time slot.

The remaining part of the paper is organized as follows. Section 2 introduces the channel models for frequency spectrum occupancy of the primary user, introducing the concept of interfering temperature and defining two models for the primary user dynamics and for the spectrum occupancy. Section 3 describes how CS-based techniques can be used for Spectrum Sensing. Section 4 describes how to estimate the main channel parameters and how to evaluate the probability to have a spectrum opportunity using these parameter estimates. Simulation results are reported both in Section 3 and in Section 4. Conclusions and final remarks are summarized in Section 5.

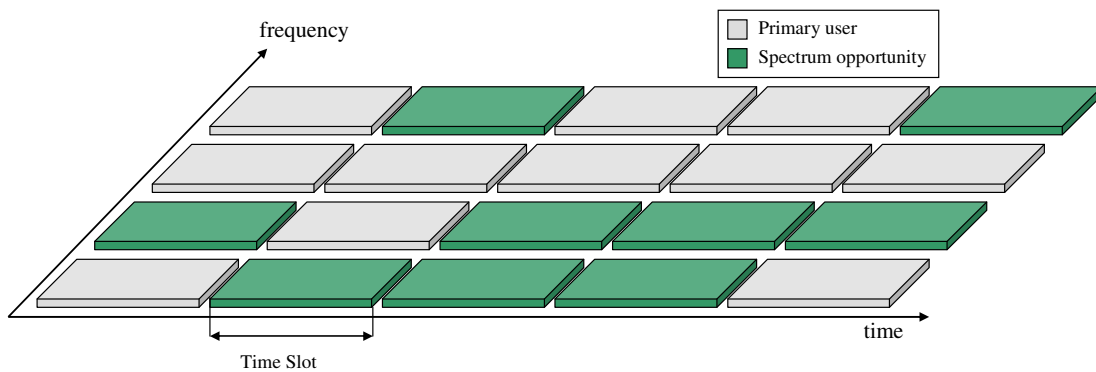


Figure 1 – Spectrum Opportunities.

2. Channel Model

As described, the cognitive radar is assumed to be the secondary user of the channel, therefore, it can use the spectrum only when it causes no harmful interference to the primary user. This requires a cognitive radar to be equipped with a spectrum sensing function, which can detect primary users' appearance and decide which portion of the spectrum is available.

Such a decision can be made according to various metrics. The traditional approach is to limit the transmitter power of interfering devices, i.e. the transmitted power should be no more than a prescribed noise floor at a certain distance from the transmitter.

However, due to the increased mobility and variability of radio frequency emitters, constraining the transmitter power becomes problematic, since unpredictable new sources of interference may appear. To address this issue, the FCC Spectrum Policy Task Force [18] has proposed a new metric on interference assessment, the interfering temperature, to enforce an interference limit perceived by receivers.

Like other representations of radio signals, instantaneous values of interference temperature would vary with time and, thus, would need to be treated statistically. In this section, we present a model for the interference temperature dynamics and the Hidden Markov Model (HMM) for channel occupancy.

2.1 Interfering Temperature

The FCC has proposed the interference temperature as a metric for interference analysis. The US Federal Communications Commission in 2002 investigated the future needs of radio frequency spectrum and the limitations of current spectrum policies, as well as develops recommendations for enhancing current policies. One recommendation was the use of an interference metric to enforce current spectrum access rights and create new opportunities for dynamic spectrum utilization [19]-[20]

The interference temperature is defined as the temperature equivalent of the RF power available at a receiving antenna per unit bandwidth [21], i.e.

$$T_I(f_C, B) = \frac{P_I(f_C, B)}{kB}, \quad (1)$$

where $P_I(f_C, B)$ is the average interference power in Watts, centered at f_C , covering bandwidth B measured in hertz, and Boltzmann's constant k is $1.38 \times 10^{-23} \text{ JK}^{-1}$.

The FCC further established an interference temperature limit, which provides a maximum amount of tolerable interference for a given frequency band at a particular location. Any secondary transmitter using this band must guarantee that its transmission plus the existing noise and interference will not exceed the interference temperature limit at a primary user. Since any transmission in the licensed band is viewed to be harmful if it would increase the noise floor above the interference temperature limit, it is necessary that a cognitive radar receiver has a reliable spectral estimate of the interference temperature. Given a particular frequency band in which the interference temperature limit is not exceeded, that band could be made available for secondary usage. If a regulatory body sets an interference temperature limit T_L for a particular frequency band with bandwidth B , then the secondary user has to keep the average interference below kBT_L . Therefore, assuming that a secondary user is operating with average power P in a band $[f_C - B/2, f_C + B/2]$, the interference temperature limit will ensure that [21]:

$$T_i(f_c, B) + \frac{LP}{kB} \leq T_L(f_c) \quad (2)$$

where L represents path loss attenuation between the secondary transmitter and the primary receiver.

2.2 Statistical model for primary user's channel occupancy

In this section, we introduce a statistical model for primary user's channel occupancy, describing the statistical model used to characterize the signal received by the cognitive radar and the statistical model for the observations at the output of the spectrum sensing detector.

The spectrum sensing module of the cognitive radar receiver periodically scans and senses multiple licensed channels to measure in each channel the interference temperature exploiting the received signal, then it compares the measured interference temperature with a predefined threshold value to evaluate if the channel is busy or free. However, due to the noise in the channel, a free channel can be classified as busy and a busy channel classified as free. In order to model the channel dynamics of the primary users, HMMs are proposed in [22]-[24]. In the context of dynamic spectrum access networks, HMMs are used to model the primary user occupancy of the channel. HMMs represent a useful tool for this problem since true occupancy states are not always known to the cognitive radar after the Spectrum Sensing process.

As discussed, the case study analysed in this work is related to an L-band surveillance radar, which shares the same frequency band with a JTDIS communication system. The frequency band used by the communication system is subdivided into N frequency channels of bandwidth B used for frequency division multiple access. As showed in Figure 1, the time axis is divided into time slots of duration Δt .

In general, a HMM is comprised of a set S_t of possible states and a set O_t of possible emissions. The possible states represent the real activity of the primary user in each frequency channel, if the primary user is transmitting at time slot t , the state is $S_t=1$, otherwise, if the channel is free, the state is $S_t=0$. However, due to the noise in the channel, a free channel can be classified as busy and a busy channel classified as free. Therefore, there are also two possible emissions, which are represented by the observation symbol O_t at the output of the spectrum sensing detector.

Figure 2 shows the HMM for spectrum occupancy in each frequency channel, in particular the lower part of the figure describes the primary user's dynamic while the upper part the secondary user's observation.

The primary user's dynamic is described by the states $S_t=0$ and $S_t=1$, and is characterized by the 2×2 state transition probability matrix \mathbf{A} , that represents the probabilities associated with changing from one state to another and it is given by

$$[\mathbf{A}]_{hk} = a_{hk} = \Pr[S_t = h | S_{t-1} = k], \quad h, k=0,1. \quad (3)$$

In each frequency channel and in each time slot, if the primary user is transmitting, the received signal at the radar receiver is given by an oscillation at that frequency whose amplitude is a Gaussian random variable (r.v.) with zero mean and variance σ_f^2 , that is

$$[\mathbf{f}_i]_n = \alpha \zeta_i \cos\left(\frac{\pi(i-1)(2n-1)}{2N}\right), \quad i, n=1, \dots, N, \quad (4)$$

where i is the frequency channel index, while n is the n -th time sample.

If the channel is free, the received signal $[\mathbf{f}_i]_n$ is zero. In each time slot, the multiband received signal is given by the combination of the signal in each frequency channel and Additive White Gaussian Noise (AWGN) with zero mean and variance σ_w^2 :

$$\mathbf{f} = \sum_{i=1}^N \mathbf{f}_i + \mathbf{w}. \quad (5)$$

The values of \mathbf{A} may be different in each frequency channel.

The spectrum occupancy is given by the Discrete Cosine Transform (DCT) of \mathbf{f} , that is

$$\mathbf{x} = \mathbf{\Psi}^T \mathbf{f}, \quad (6)$$

where $\mathbf{\Psi}$ is the DCT matrix whose elements are given by

$$[\mathbf{\Psi}]_{i,j} = \zeta_i \cos\left(\frac{\pi(i-1)(2j-1)}{2N}\right), \quad i, j=1, \dots, N. \quad (7)$$

In (4) and (7) the values of ζ_i are given by

$$\zeta_i = \begin{cases} 1/\sqrt{N}, & i = 1 \\ \sqrt{2/N}, & 2 \leq i \leq N \end{cases} \quad (8)$$

Note that, in this work, without any lack of generality, we can consider real signals, instead of the complete complex signals. In fact, to monitor the spectrum occupancy of the primary users and to reduce the cost of the receiver further, it is not necessary to process the In-Phase (I) and Quadrature (Q) components of the received signal, but only one of them. Figure 3 shows the squared absolute value of \mathbf{x} , that is the channel occupancy evolution during an observation time composed of ten time slots Δt . The channel is composed of $N=256$ frequency bands and the Signal to Noise Ratio, defined as $\text{SNR} = \sigma_f^2 / \sigma_w^2$, is 20dB.

To evaluate the channel occupancy evolution it is necessary to perform the DCT of the received time samples every Δt seconds. When the frequency band to be monitored tends to be very wide and/or the time slot Δt tends to be very short, it should be very difficult to collect the N time samples at the Nyquist-rate. In Section 3, we study how CS may be used to alleviate this hardware constraint.

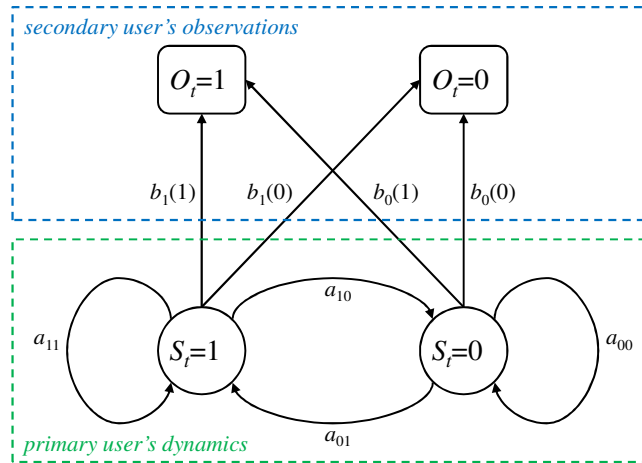


Figure 2 – Hidden Markov Model representation for spectrum occupancy.

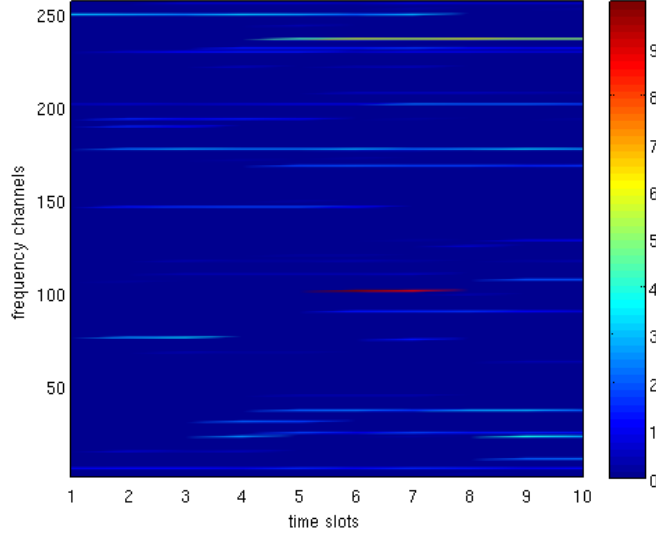


Figure 3 - Channel occupancy evolution in ten time slots, $N=256$, $\text{SNR}=20\text{dB}$.

In the open literature, there are several Spectrum Sensing techniques to recognize if the channel is occupied by the primary user, such as the energy detector, feature detector or matched filtering detection techniques [25]. In particular, at each time slot, the cognitive radar records an observation symbol O_t depending upon the following conditions:

$$\begin{cases} O_t = 0, & \text{if } T_t(t) \leq T_L \\ O_t = 1, & \text{if } T_t(t) > T_L \end{cases} \quad (9)$$

The radar periodically makes the observations and records an observation sequence $\mathbf{O}=[O_1 \dots O_T]$ over a period of T time slots. The transitions from the states S_t to the observations O_t are described by the 2×2 emission probability matrix \mathbf{B} , which represents the probabilities associated with obtaining a certain output given that the model is currently in a true state s_t :

$$[\mathbf{B}]_{hk} = b_h(k) = \Pr[O_n = h | S_n = k]. \quad (10)$$

The emission probability matrix \mathbf{B} is related to the Receiver Operating Characteristic (ROC) of the Spectrum Sensing detector. As a matter of fact, $b_0(1)$ is the probability of false alarm, that is the probability to classify a free channel as busy, whereas $b_1(0)$ is the probability of miss detection, that is the probability to classify a busy channel as free. Clearly, $b_0(0)=1-b_0(1)$ and $b_1(1)=1-b_1(0)$. These probabilities depend on the channel

noise, the kind of signal emitted by the primary user and the spectrum sensing detector used at the cognitive radar receiver, that is on the specific characteristics of the systems that share the same channel. Knowing these characteristics, the elements of \mathbf{B} can be calculated or evaluated through Monte Carlo simulations. Hence, without loss of generality, hereafter we assume that \mathbf{B} is known. Section 4 will describe how to estimate the channel parameters from the observation sequence \mathbf{O} and how to exploit these estimates to minimize the interference between the radar and the communication system.

3. Compressed Spectrum Sensing

In this section, after a brief introduction to the principles of Compressed Sensing (CS), we focus on its application to Spectrum Sensing, that will be referred to as Compressed Spectrum Sensing (CSS). For more details on CS we refer the reader to [15]-[17] and references therein.

CS is a signal processing methodology for signal recovery from highly incomplete information.

The central results state that a sparse vector¹ $\mathbf{x} \in \mathbb{R}^N$ can be recovered from a small number of linear measurements $\mathbf{y} = \mathbf{H}\mathbf{x} \in \mathbb{R}^K$, $K \ll N$ (or $\mathbf{y} = \mathbf{H}\mathbf{x} + \mathbf{w}$ when there is measurement noise) by solving a convex program [15]-[17]. To make this possible, CS relies on two principles: sparsity, which pertains to the signal of interest, and incoherence, which pertains to the sensing modality. Considering the real signal $\mathbf{f} \in \mathbb{R}^N$ defined in (5) and being $\Psi = [\psi_1 \dots \psi_N]$ an orthonormal basis (e.g. the DCT), then the representation of \mathbf{f} on the basis Ψ is given by $\mathbf{f} = \Psi\mathbf{x}$, where \mathbf{x} is the sparse coefficient vector. Given a set of vectors $[\varphi_1, \dots, \varphi_K]$ and denoting with Φ the $K \times N$ sensing matrix whose rows are the φ_k 's, the measures are collected by means of linear functionals $\mathbf{y} = \Phi\mathbf{f} = \Phi\Psi\mathbf{x} \in \mathbb{R}^K$ [15]-[16]. The interest is in undersampled situations in which the number K of available measurements is much smaller than the dimension N of the signal \mathbf{f} . The process of recovering the $K \times 1$ vector $\mathbf{x} = \Psi^T\mathbf{f}$ from the $N \times 1$ measurement vector $\mathbf{y} = \Phi\mathbf{f}$ is, in general, ill-posed when $K < N$. However, if \mathbf{x} is s -sparse, then the problem can be solved provided $K \geq s$. A necessary and sufficient condition for this problem is that, for some small $\delta > 0$, the matrix $\mathbf{H} = \Phi\Psi$ satisfies the Restricted Isometry Property (RIP) [26]:

¹ A vector is s -sparse if it has at most s nonzero entries.

$$(1 - \delta) \|\mathbf{x}\|_2 \leq \|\mathbf{H}\mathbf{x}\|_2 \leq (1 + \delta) \|\mathbf{x}\|_2. \quad (11)$$

The RIP implies that matrix \mathbf{H} must preserve the length of s -sparse vectors. A related condition to RIP is referred as *incoherence*. The coherence between the measurement matrix Φ and the representation matrix Ψ measures the largest correlation between any two columns of these matrix and is defined as

$$\mu(\Phi, \Psi) = \sqrt{N} \max_{1 \leq k, j \leq N} |\langle \phi_k, \psi_j \rangle|. \quad (12)$$

It can be shown [15]-[17] that $\mu(\Phi, \Psi) \in [1, \sqrt{N}]$. The design of a measurement matrix Φ such that $\mathbf{H} = \Phi\Psi$ has the RIP requires that all possible combination of s nonzero entries on the vector \mathbf{x} of length N have to satisfy (11). However, both the RIP and incoherence can be achieved with high probability by designing Φ as a random matrix [15].

Now, it is natural to attempt to recover \mathbf{x} by solving the following optimization problem:

$$\hat{\mathbf{x}} = \arg \min_{\mathbf{x} \in \mathbb{R}^N} \|\mathbf{x}\|_0, \quad \text{s.t. } \Phi\Psi\mathbf{x} = \mathbf{y}. \quad (13)$$

In the literature, this minimization is referred as the Basis Pursuit (BP) method, which, for real valued signals, can be recast as a linear programming problem. The BP method is guaranteed to find a reconstruction of a s -sparse signal if there is no measurement noise. However, in the presence of measurement noise, its influence on the signal reconstruction can be minimized by applying the Basis Pursuit De-Noising (BPDN) method which finds a solution of the following problem [27]:

$$\hat{\mathbf{x}} = \arg \min_{\mathbf{x} \in \mathbb{R}^N} \|\mathbf{x}\|_1, \quad \text{s.t. } \|\mathbf{y} - \Phi\Psi\mathbf{x}\|_2 \leq \sigma, \quad (14)$$

where the positive parameter σ is an estimate of the noise level in the data. The case $\sigma=0$ corresponds to the basis pursuit problem. The BPDN method can be solved by means of linear programming algorithms.

As previously discussed, when the frequency spectrum of the user radiating in the same channel as the cognitive radar is a sparse signal, it is possible to apply CS ideas to Spectrum Sensing. For the problem at hand, the representation matrix Ψ is the DCT, whose elements are defined in (7). In this work, we consider two kind of measurement matrices Φ , the first one is the Gaussian matrix, which is formed by sampling independent and identically distributed (IID) entries from the normal distribution with zero mean and variance $1/K$:

$$[\Phi]_{i,j} \sim N(0, 1/K), \quad i=1, \dots, K; j=1, \dots, N. \quad (15)$$

The second measurement matrix is the Spiky matrix given by randomly selecting K rows of the $N \times N$ identity matrix. The latter case is the more interesting because, from the definition of this matrix, the measurement vector \mathbf{y} is obtained by simply selecting K samples of \mathbf{f} at random. The use of CS allows to use an ADC with a rate of $K/\Delta t$ instead of an ADC with rate $N/\Delta t$. For the physical implementation of the CS filters, we refer the reader to [28]-[30].

Figure 4 shows the channel occupancy evolution of Figure 3 recovered using the Gaussian measurement matrix, whereas Figure 5 shows the results obtained using the Spiky measurement matrix. In both cases $K=N/2$ and $\text{SNR}=20\text{dB}$.

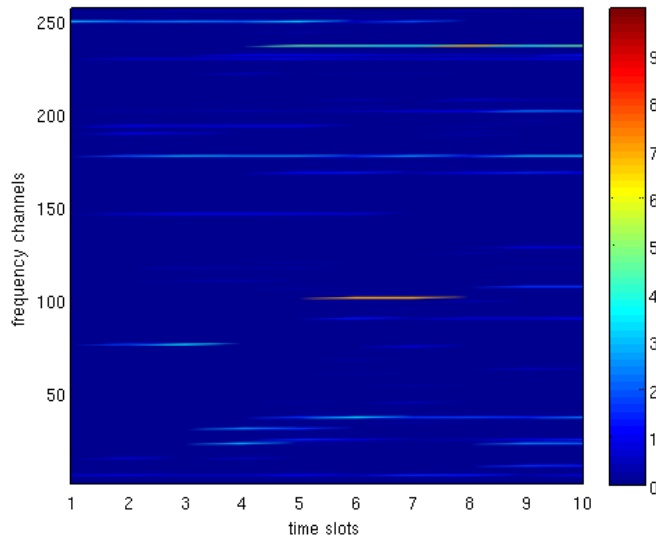


Figure 4 - Channel occupancy evolution recovered using the Gaussian measurement matrix, $K=N/2$.

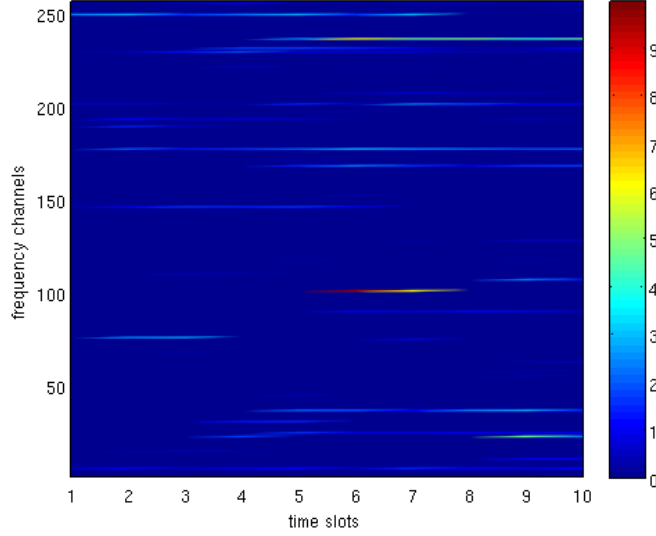


Figure 5 - Channel occupancy evolution recovered using the Spiky measurement matrix, $K=N/2$.

Figure 6 shows the Root Mean Square Error (RMSE) after the reconstruction of the channel occupancy signal. The RMSE measures the error in reconstructing \mathbf{x} using CSS w.r.t. the reference signal estimated with all the N samples, that is

$$\text{RMSE} = \sqrt{\frac{1}{MH} \sum_{h=1}^H \sum_{m=1}^M |\hat{\mathbf{x}}_m^{(h)} - \mathbf{x}_m^{(h)}|^2}, \quad (16)$$

where m and h are the time slot and the Monte Carlo run indexes, respectively.

The results are shown as a function of K (percentage of N) for both the measurements matrices and for different values of the Signal-to-Noise power ratio (SNR). The performance results obtained using the two matrices are about the same. It is also apparent that, in the absence of noise, it is possible to reconstruct the signal of interest using a very low number of samples (30% of N). However, as the noise power increases we need more samples to minimize the influence of the noise on the signal reconstruction. Anyway, when the SNR tends to be high, the signal can be almost perfectly reconstructed using fewer samples (40% of N). From our analysis (see Figures 5-6), the RMSE in reconstructing the signal is strictly related to the fact that, when the channel is busy, we need a high number of samples to reconstruct the whole spectrum with high precision. However, in this case, even if we use a low number of samples, a busy channel is always recognized to be busy. As a matter of fact, when performing the cognitive spectrum sensing function, we are not interested on reconstructing the whole

spectrum with high accuracy, but rather on deciding which channels are busy. With regard to this latter operation, we apply the classical energy detector technique [31], which compares the squared value of each element of the spectrum occupancy vector $r_k=x_k^2$ with a threshold ζ to evaluate if the channel is busy/free. We evaluated the percentage of error in the decision on the channel occupancy applying the same threshold to the reconstructed signal as a function of K .

According to the signal model described in Section 2.2, in the two hypotheses the elements of the vector \mathbf{x} are given by

$$\begin{cases} x_k \sim N(0, \sigma_w^2), & H_0 \\ x_k \sim N(0, \sigma_f^2 + \sigma_w^2), & H_1 \end{cases} \quad (17)$$

where σ_f^2 is the variance of the primary user's signal and σ_w^2 is the variance of the noise. Being the squared value of a Gaussian r.v. a χ^2 r.v. with one degree of freedom, the binary hypothesis test is given by

$$\begin{cases} r_k \sim \sigma_w^2 \chi_1^2 & H_0 \\ r_k \sim (\sigma_f^2 + \sigma_w^2) \chi_1^2 & H_1 \end{cases} \quad (18)$$

Indicating with P the upper incomplete gamma function, the probability of detection P_D and the probability of false alarm P_{FA} are given by

$$P_D = \Pr\{r_k \geq \zeta \mid H_1\} = \Pr\left\{\chi_1^2 \geq \frac{\zeta}{\sigma_f^2 + \sigma_w^2}\right\} = P\left(\frac{\zeta}{2(\sigma_f^2 + \sigma_w^2)}, \frac{1}{2}\right) \quad (19)$$

$$P_{FA} = \Pr\{r_k \geq \zeta \mid H_0\} = \Pr\left\{\chi_1^2 \geq \frac{\zeta}{\sigma_w^2}\right\} = P\left(\frac{\zeta}{2\sigma_w^2}, \frac{1}{2}\right). \quad (20)$$

In our Monte Carlo simulations, we evaluated the percentage of error in the decision on the channel occupancy (i.e. if a free channel is declared as busy and vice versa), the results are shown in Figure 7 when ζ is fixed for a probability of detection of 0.8. Note that in a radar detector the probability of false alarm is fixed to a desired value and the probability of detection is maximized according to the Newman-Pearson criterion. It is

convenient to keep constant the probability of false alarm to a low value because a false alarm is more problematic than a miss detection. As a matter of fact, for each detection a lot of radar procedures, such as target tracking and target identification, are activated, if there are a lot of false alarms a great portion of the system memory and computational capabilities are occupied for the tracking of inexistent targets. For the problem of Spectrum Sensing, being the radar the secondary user of the channel, the more problematic event is the miss detection, that is when the channel is declared as free and the primary user is transmitting. For this reason, it is convenient to fix the probability of detection to a desired value and minimize the probability of false alarm. Note also that in this case, being the threshold dependent on the SNR, the probability of false alarm depends on the SNR. In particular, in the simulation the probability of detection has been fixed to 0.8 for each value of SNR, while the corresponding probability of false alarm according to (20) is 0.01 for SNR=20dB and 0.15 for SNR=15dB.

The results in Figure 7 show that, when the SNR is sufficiently high, the error percentage is reasonably low, which means that the busy/free decision can still be carried out on the signal reconstructed with few samples (<30% of N), even if the signal is not accurately reconstructed.

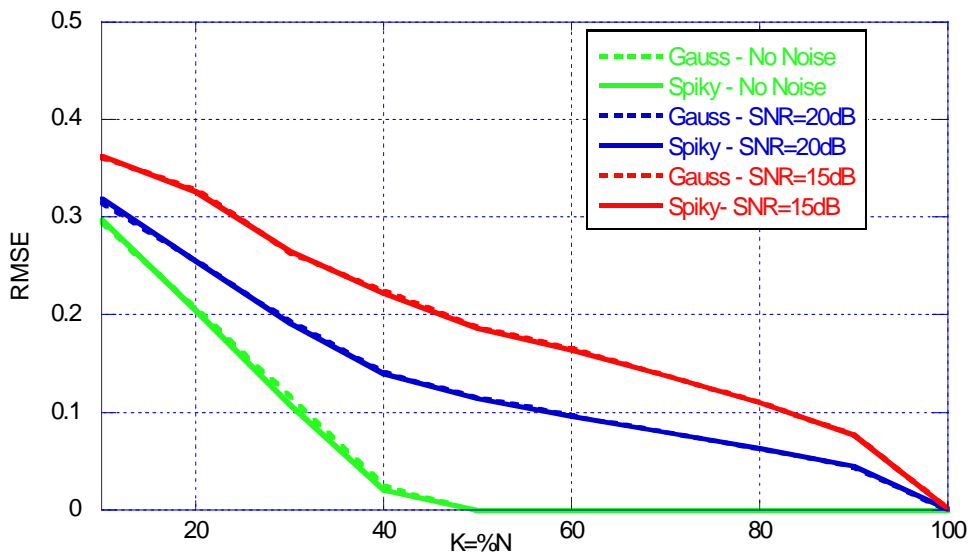


Figure 6 - RMSE for channel occupancy reconstruction as a function of K (percentage of N) for different SNR values.

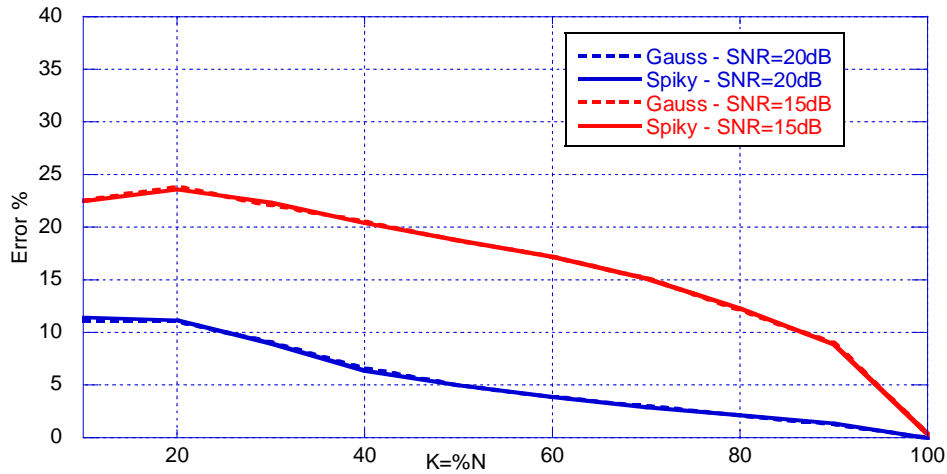


Figure 7 - Error percentage on the decision of channel occupancy as a function of K (percentage of N) for different SNR values.

4. Channel Monitoring for Spectrum Sharing

In the previous Section, we showed how the spectrum sensing detector exploits the received signal to obtain the observation symbols O_t used to evaluate if the channel is busy or free at time slot t . To detect the presence of the primary user, the spectrum sensing detector must process the time signal received in the whole time slot. Considering that the Pulse Repetition Interval (PRI) of the radar system and the time slot of the communication system are of the same time duration, in each channel at the time of transmitting (i.e. at the beginning of each PRI), the radar could not be able to measure if the frequency channel is effectively occupied by the communication system.

For minimizing interference to primary users while making the most out of the spectrum opportunities, the cognitive radar should keep track of variations in spectrum availability and, exploiting the history of the spectrum usage information, should make predictions of the future profile of the spectrum. Therefore, the cognitive radar system analyses the behaviour of the primary user in the frequency channel and, exploiting the time history of the channel occupancy (i.e. a sequence of observation symbols), it can evaluate the probability to have a spectrum opportunity at the beginning of each PRI, i.e. the probability that the monitored frequency channel is free at the time of transmitting.

In this Section, we describe how to estimate the channel parameters that model the behaviour of the primary user in a frequency channel and how to exploit this estimate to evaluate the probability to have a spectrum opportunity.

4.1 Channel parameters estimation

As discussed in Section 2.2, the statistical parameters that describe each frequency channel are the state transition probability matrix \mathbf{A} , the emission probability matrix \mathbf{B} , and the initial state distribution $\boldsymbol{\pi}=\{\pi_i\}$, defined as

$$\pi_i = \Pr[s_1 = S_i], \quad i=0,1. \quad (21)$$

Matrix \mathbf{B} is related to the ROC of the spectrum sensing detector and, as discussed in Section 2.2, is assumed to be a-priori known. Hence, the problem of channel parameter estimation is to determine a method to estimate the model parameters \mathbf{A} and $\boldsymbol{\pi}$ using a finite observation sequence $\mathbf{O}=[O_1 \dots O_T]$ of T elements. The observation sequence used to adjust the model parameters is called training sequence since it is used to “train” the HMM. There is no way to solve analytically this problem [32]. In fact, given any finite observation sequence as training data, there is no optimal way of estimating the model parameters. However, the most widely adopted iterative procedure is the Baum-Welch method, which is closely related to the Expectation-Maximization (EM) method [23], [24], [32], [33]. The Baum-Welch method selects the parameters \mathbf{A} and $\boldsymbol{\pi}$ such that $\Pr[\mathbf{O}|\mathbf{A},\boldsymbol{\pi}]$ is locally maximized.

In order to describe the iterative procedure for estimation of the HMM parameters, first we must define some useful variables. First consider the forward variable $\alpha_t(i)$ defined as

$$\alpha_t(i) = \Pr[O_1 O_2 \dots O_t, s_t = S_i | \mathbf{A}, \boldsymbol{\pi}] \quad (22)$$

That is the probability of the partial observation sequence $O_1 \dots O_t$ and state S_i at time t , given the channel parameters \mathbf{A} and $\boldsymbol{\pi}$. The forward variable can be inductively calculated initializing

$$\alpha_1(i) = \pi_i b_i(O_1), \quad i=0,1, \quad (23)$$

and iterating

$$\alpha_{t+1}(j) = \left[\sum_{i=0}^1 \alpha_t(i) a_{ij} \right] b_j(O_{t+1}), \quad 1 \leq t \leq T-1, j=0,1. \quad (24)$$

In a similar manner, the backward variable $\beta_t(i)$ is defined as

$$\beta_t(i) = \Pr[O_{t+1}O_{t+2}\dots O_T \mid s_t = S_i, \mathbf{A}, \boldsymbol{\pi}], \quad (25)$$

that is the probability of the partial observation sequence from $t+1$ to T , given state S_i at time t and the channel parameters \mathbf{A} and $\boldsymbol{\pi}$.

Similarly, $\beta_t(i)$ can be solved inductively initializing

$$\beta_T(i) = 1, \quad i=0,1 \quad (26)$$

and iterating

$$\beta_t(i) = \sum_{j=0}^1 a_{ij} b_j(O_{t+1}) \beta_{t+1}(j), \quad t=T-1, \dots, 1; i=0,1. \quad (27)$$

Another important variable is the probability

$$\gamma_t(i) = \Pr[s_t = S_i \mid \mathbf{O}, \mathbf{A}, \boldsymbol{\pi}], \quad (28)$$

that is the probability of being in state S_i at time t , given the observation sequence \mathbf{O} and the channel parameters \mathbf{A} and $\boldsymbol{\pi}$. This probability can be expressed simply in terms of the forward-backward variables:

$$\gamma_t(i) = \frac{\alpha_t(i) \beta_t(i)}{\sum_{j=0}^1 \alpha_t(j) \beta_t(j)}, \quad i=0,1. \quad (29)$$

Concluding, for the iterative estimation of the HMM parameter we must define the probability of being in state S_i at time t and state S_j at time $t+1$, given the observation sequence \mathbf{O} and the channel parameters \mathbf{A} and $\boldsymbol{\pi}$

$$\xi_t(i, j) = \Pr[s_t = S_i, s_{t+1} = S_j \mid \mathbf{O}, \mathbf{A}, \boldsymbol{\pi}], \quad i, j=0,1. \quad (30)$$

From the definitions of the forward and backward variables, we can write (30) in the form [32]:

$$\xi_t(i, j) = \frac{\alpha_t(i) a_{ij} b_j(O_{t+1}) \beta_{t+1}(j)}{\sum_{i=0}^1 \sum_{j=0}^1 \alpha_t(i) a_{ij} b_j(O_{t+1}) \beta_{t+1}(j)}, \quad i, j=0,1. \quad (31)$$

It is easy to verify by using (30) that the probability in (28) is given by

$$\gamma_t(i) = \sum_{j=0}^1 \xi_t(i, j), \quad i=0,1. \quad (32)$$

If we sum $\gamma_t(i)$ over the time index t , we get a quantity which can be interpreted as the expected (over time) number of times that state S_i is visited, or equivalently, the expected number of transitions made from state S_i . Similarly, summation of $\xi_t(i, j)$ over t (from $t=1$ to $t=T-1$) can be interpreted as the expected number of transitions from state S_i to state S_j . Using (29) and (31) with the concept of counting event occurrences, it is possible to define a method to iteratively estimate the parameters of an HMM.

Considering that the ij -th element of the state transition probability matrix \mathbf{A} can be considered as the ratio of the expected number of transitions from state S_i to state S_j and the expected number of transitions made from state S_i , it is possible to estimate the elements of \mathbf{A} by using the following equation

$$\hat{a}_{ij} = \frac{\sum_{t=1}^{T-1} \xi_t(i, j)}{\sum_{t=1}^{T-1} \gamma_t(i)}, \quad i, j=0,1. \quad (33)$$

Similarly, the initial state distribution π_i can be considered as the expected number of times in state S_i at time $t=1$, therefore we can estimate $\boldsymbol{\pi}$ using

$$\hat{\pi}_i = \gamma_1(i), \quad i=0,1. \quad (34)$$

If we define the current channel parameters \mathbf{A} and $\boldsymbol{\pi}$ and we use them to compute (29) and (31), and we define the re-estimated channel parameters as $\hat{\mathbf{A}}$ and $\hat{\boldsymbol{\pi}}$, determined from (33) and (34), then it has been proven in [34] and [35] that the model

described by $\hat{\mathbf{A}}$ and $\hat{\boldsymbol{\pi}}$ is more likely than the model described by \mathbf{A} and $\boldsymbol{\pi}$, in the sense that $\Pr[\mathbf{O}|\hat{\mathbf{A}}, \hat{\boldsymbol{\pi}}] > \Pr[\mathbf{O}|\mathbf{A}, \boldsymbol{\pi}]$, i.e. we have found a new set of channel parameters from which the observation sequence is more likely to have been produced.

Based on the above procedure, if we iteratively use $\hat{\mathbf{A}}$ and $\hat{\boldsymbol{\pi}}$ in place of \mathbf{A} and $\boldsymbol{\pi}$ and repeat the re-estimation, we can improve the probability of \mathbf{O} being observed from the model until some limiting point is reached. The final result of this procedure is a maximum likelihood (ML) estimate of the HMM [32]. This procedure is called Baum-Welch method and it is summarized in Table 1.

<p>Input: observation sequence $\mathbf{O}=O_1\dots O_N$ initialize \mathbf{A} and $\boldsymbol{\pi}$ for $k=1:\text{MaxIter}$ calculate $\gamma_n(i)$ and $\zeta_n(i,j)$ from \mathbf{A} and $\boldsymbol{\pi}$ estimate $\hat{\mathbf{A}}$ and $\hat{\boldsymbol{\pi}}$ from $\gamma_n(i)$ and $\zeta_n(i,j)$ substitute \mathbf{A} and $\boldsymbol{\pi}$ with $\hat{\mathbf{A}}$ and $\hat{\boldsymbol{\pi}}$. end Output: estimate of \mathbf{A} and $\gamma_n(i), n=1,\dots,N; i=0,1.$</p>

Table 1 - Baum-Welch procedure.

By Monte Carlo simulation, we evaluated that using 30 iterations the algorithm converges to a stable estimate of \mathbf{A} and $\boldsymbol{\pi}$. Figure 8 shows the Root Mean Square Error (RMSE) of the estimation of the elements of \mathbf{A} as a function of the number of elements of the observation sequence T . These results have been obtained through 10^3 Monte Carlo runs by random generating a_{00} and a_{11} as independent and identically distributed (IID) random variables, uniformly distributed in $[0,1]$. Considering that (29) and (31) measure the expected number of transitions from one state to the other, it is clear that in order to have a good estimate of \mathbf{A} , we need an high value of T , when the number of elements of the observation sequence is too low the estimate of \mathbf{A} is biased.

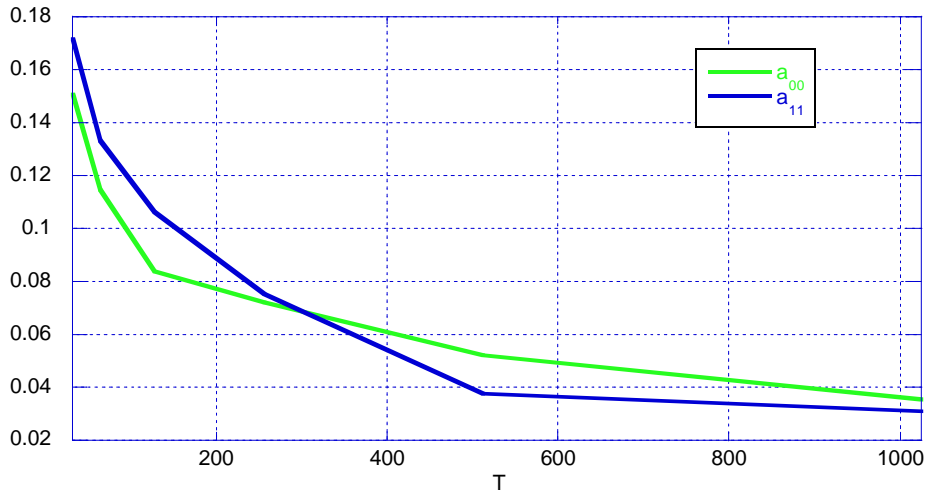


Figure 8 - RMSE in the estimation of \mathbf{A} as a function of the number of elements of the observation sequence.

4.2 Probability of Spectrum Opportunity

In the previous Section, we showed how to estimate the channel parameters using a finite observation sequence. In this section, we show how the cognitive radar exploits these estimates to avoid interference with the primary user. We also show some simulation results that highlight how the proposed methodology can provide good radar performance in the presence of the user and low impact on the performance of the primary user by the presence of the radar.

As discussed, in the analysed scenario, at the time of transmitting the cognitive radar is not able to evaluate instantaneously if the operating channel is free or busy. However, using the channel parameter estimates obtained from the last T channel observations, the cognitive radar can calculate the probability that at the time of transmitting the channel is free, i.e. the probability to have a spectrum opportunity. If this probability is sufficiently high, the cognitive radar transmits, otherwise it does not transmit.

Figure 9 shows how the radar processes the continuous sequence of observations at the output of the spectrum-sensing detector. Since the estimation of \mathbf{A} and $\gamma_l(i)$ is time consuming, the radar receiver performs these estimates using non-overlapping blocks of T elements, in each block the initialization is performed using the channel parameter estimates of the previous block. As showed in Figure 9, the channel parameter estimates performed in each block are used to evaluate the probability to have a spectrum opportunity using a sliding window that collects the last T observations received in the previous time slots.

There are T sliding windows for each block, in particular in the k -th sliding window, using the estimate of \mathbf{A} and fixing $\pi_i = \gamma_k(i)$, the signal processor of the radar evaluates the forward and the backwards variables using (23)-(27). Therefore, similarly to (29), evaluates the probability that the last observation in the sliding window corresponds to the channel state S_i , that is

$$\gamma(i) = \frac{\alpha_T(i)\beta_T(i)}{\sum_{j=0}^1 \alpha_T(j)\beta_T(j)}, \quad i=0,1. \quad (35)$$

This probability is used to evaluate the probability to have a spectrum opportunity:

$$p_{SO} = \gamma(0)a_{00} + \gamma(1)a_{01}, \quad (36)$$

i.e. the probability that in the previous time slot the channel was free and in the current time slot it remains free plus the probability that in the previous time slot the channel was busy and in the current time slot it becomes free. The signal processor compares the probability to have a spectrum opportunity with a threshold λ , and transmits only if the probability is greater than λ .

There are two kinds of errors. The first one, e_0 , is the event in which the cognitive radar does not transmit and the channel is free, i.e. the probability to lose a spectrum opportunity. The other kind of error, e_1 , is the case in which the radar transmits and the channel is occupied by the primary user, i.e. the probability to have a collision.

Figure 10 shows the probability of these two errors as a function of the threshold λ , this graph can be used to tune the cognitive radar to the desired performance. These results have been obtained through 10^3 Monte Carlo runs by random generating a_{00} and a_{11} as independent random variables uniformly distributed in the range $[0,1]$.

It is clear that when threshold λ is zero, the radar is always transmitting, therefore the probability of e_1 coincides with the probability that the channel is busy, that for the matrix \mathbf{A} that we used in our simulation, is 0.5. Similarly, when the threshold λ is one, the radar never transmits and the probability of e_0 coincides with the probability that the channel is free, that in our particular case, is 0.5.

Figure 11 shows the probability to lose a spectrum opportunity and the probability to have a collision as a function of time, observing the performance of the system for 9246 time slots (i.e. 9 blocks of 1024 elements). These results have been obtained through 10^3 Monte Carlo runs, generating a_{00} and a_{11} as IID random variables uniformly distributed in $[0,1]$ and fixing the threshold λ to 0.65.

The simulation results show how the performance of a cognitive radar that adopts the proposed methodology are constant during the time and much better than the performance of the non cognitive radar that always transmits ignoring the presence of the primary user and than the radar that never transmits to avoid interference with the primary user of the channel.

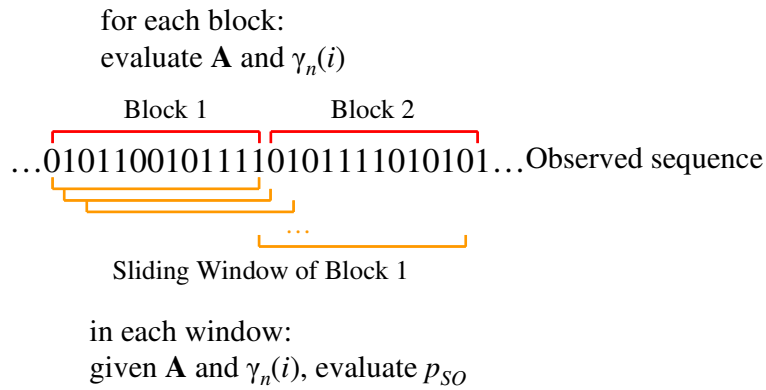


Figure 9 - How to process the observed sequence.

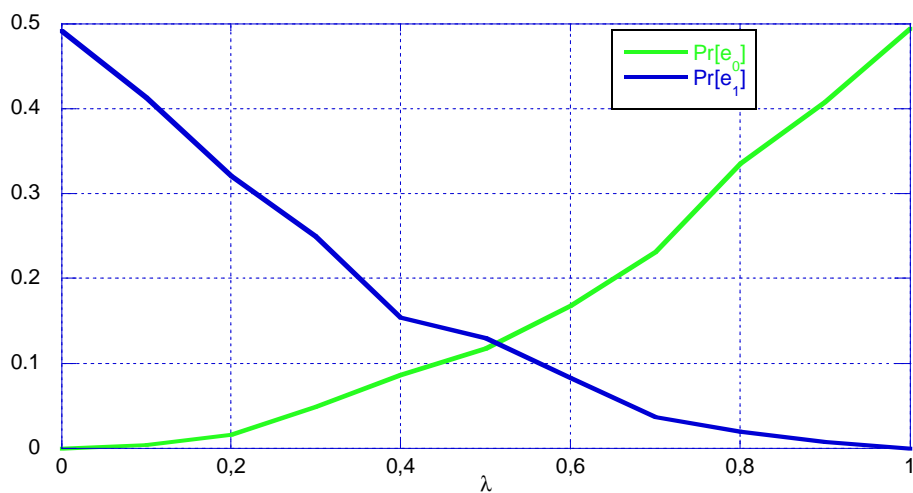


Figure 10 - Probabilities of e_0 and e_1 as a function of λ .

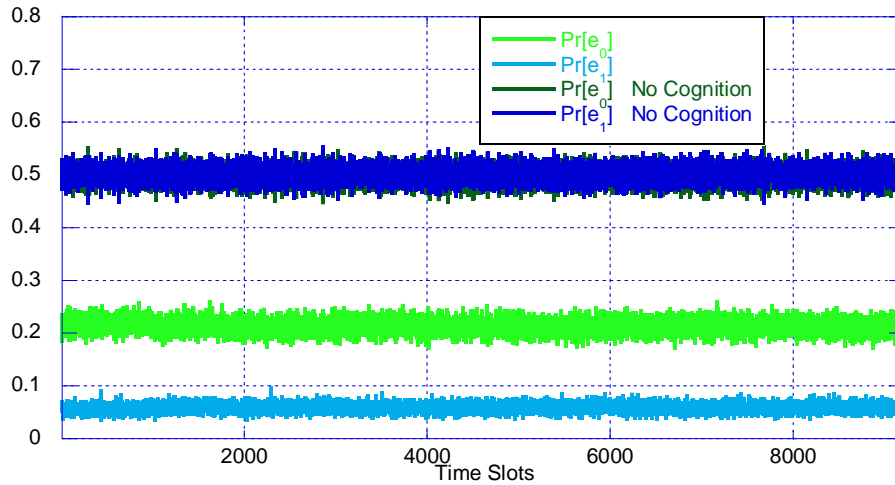


Figure 11 - Probabilities of e_0 and e_1 as a function of time.

5. Conclusions

Since the availability of frequency spectrum for radar sensors continuously diminished and fragmented, next generation radar systems should be able to operate in spectrally dense environments, coexisting with other systems operating in the same frequency channel. For this reason, an important system requirement is the ability to recognize and react to the behaviour of other users radiating in the same operational environment that, in turn, leads to the need of new methodologies and techniques, based upon cognition as enabling technology. The cognitive methodology to reduce mutual interference between the radar and the other radiating elements is based on two main concepts: Spectrum Sensing, that has the goal to recognize the frequencies used by other systems using the same spectrum in real time, and Spectrum Sharing, that has the goal to limit interference from the radar to other services and vice versa.

This paper focus on two main topics, the role that Compressed Sensing in Spectrum Sensing and the problem of channel parameter estimation for Spectrum Sharing. In particular, we demonstrate that CS techniques can provide a significant reduction in acquisition time, reducing the cost for high resolution Analog-to-Digital converters with large dynamic range and high speed signal processors. In the specific application, where the goal is not reconstructing the whole spectrum with high accuracy, but rather to decide which are the busy channels in the considered band, the results show that, when the SNR is sufficiently high, the error percentage on the busy/free decision can be low already using less than 30% of the total samples of the original signal. This mitigates the hardware constraints of conventional spectrum sensing techniques and allows to reduce the sampling rate. Moreover, this paper describes a technique to estimate the channel

parameters that model the behaviour of the primary user of the channel, and propose a cognitive method that, exploiting these estimates, enables a radar to operate in a spectrally dense environment. The performance of the cognitive radar is evaluated in terms of probability to lose a spectrum opportunity and probability to have a collision with the primary user of the channel. The numerical results suggest that the proposed cognitive algorithm lowers the mutual interference between the radar and the primary users.

REFERENCES

- [1] M. Wicks, "Spectrum crowding and Cognitive Radar," *2nd International Workshop on Cognitive Information Processing (CIP2010)*, Elba Island, Italy, June 2010.
- [2] M. Wicks, "Cognitive radar: A way forward," *IEEE International Radar Conference (RADAR 2011)*, May 2011.
- [3] ITU-R Resolution 229, "Use of the bands 5150-5250 MHz, 5250-5350 MHz and 5470-5725 MHz by the mobile service for the implementation of wireless access systems including radio local area networks", 2012.
- [4] ITU-R RECOMMENDATION M.1652, "Dynamic frequency selection (DFS) in wireless access systems including radio local area networks for the purpose of protecting the radio determination service in the 5 GHz band", 2003.
- [5] U.S. Department of Commerce, "An Assessment of the Near-Term Viability of Accommodating Wireless Broadband Systems in the 1675-1710 MHz, 1755-1780 MHz, 3500-3650 MHz, and 4200-4220 MHz, 4380-4400 MHz Bands", 2010.
- [6] E. Obregon, K.W. Sung, J. Zander, "Secondary Access to the Radar Spectrum Bands: Regulatory and Business Implications", *24th European Regional Conference of the International Telecommunications Society*, Florence, Italy, 2013.
- [7] S. Haykin, "Cognitive radar: A way of the future," *IEEE Signal Process. Mag.*, Vol. 23, No. 1, pp. 30-40, Jan. 2006.
- [8] S. Haykin, X. Yanbo, P. Setoodeh, "Cognitive Radar: Step toward Bridging the Gap between Neuroscience and Engineering," *Proceedings of the IEEE*, vol.100, no.11, pp.3102-3130, Nov. 2012
- [9] S. Haykin, *Cognitive Dynamic Systems: Perception-action Cycle, Radar and Radio*, Cambridge University Press, 2012.
- [10] G.T. Capraro, A. Farina, H. Griffiths, M.C. Wicks, "Knowledge-based radar signal and data processing: a tutorial review," *IEEE Signal Process. Mag.*, Vol. 23, No. 1, pp. 18-29, Jan. 2006.
- [11] P. Stinco; M. Greco; F. Gini; M. Rangaswamy; "Ambiguity function and Cramer-Rao bounds for universal mobile telecommunications system-based passive coherent location systems," *Radar, Sonar & Navigation, IET*, vol.6, no.7, pp.668-678, August 2012
- [12] P. Stinco; M. Greco; F. Gini; A. Farina; "Posterior Cramér-Rao Lower Bounds for Passive Bistatic Radar Tracking with Uncertain Target Measurements" *Special Issue on Sensor Array Processing, Signal Processing, Signal Processing*, Vol. 93, No. 12, pp. 3528-3540, December 2013.
- [13] Y. Hur, J. Park, W. Woo, K. Lim, C. Lee, H. Kim, J. Laskar, "A wideband analog multi-resolution spectrum sensing (MRSS) technique for cognitive radio (CR) systems," *in*

- Proc. IEEE Int. Symp. Circuits and Systems*, Island of Kos, Greece, May 2006, pp. 4090–4093.
- [14] Y. Yuan, P. Bahl, R. Chandra, P. A. Chou, J. I. Ferrell, T. Moscibroda, S. Narlanka, Y. Wu, “KNOWS: Cognitive radio networks over white spaces,” in *Proc. IEEE Int. Symposium on New Frontiers in Dynamic Spectrum Access Networks*, Dublin, Ireland, Apr. 2007, pp. 416–427.
- [15] E.J. Candes, M.B. Wakin; “An Introduction To Compressive Sampling,” *Signal Processing Magazine, IEEE*, Vol. 25, No. 2, pp. 21-30, March 2008.
- [16] D.L. Donoho; “Compressed sensing,” *Information Theory, IEEE Transactions on*, Vol. 52, No. 4, pp. 1289-1306, April 2006.
- [17] D.L. Donoho, X. Huo; “Uncertainty principles and ideal atomic decomposition,” *Information Theory, IEEE Transactions on*, Vol. 47, No. 7, pp. 2845-2862, Nov 2001.
- [18] Federal Communications Commission, Notice of Inquiry and Notice of Proposed Rulemaking: In the matter of Establishment of an Interference Temperature Metric to Quantify and Manage Interference and to Expand Available Unlicensed Operation in Certain Fixed, Mobile and Satellite Frequency Bands, ET Docket No. 03-237; November 28, 2003.
- [19] D. Cabric, S. Mishra, R. Brodersen, “Implementation issues in spectrum sensing for cognitive radios,” in *Proc. Asilomar Conf. on Signals, Systems and Computers*, Vol. 1, Pacific Grove, California, USA, Nov. 2004, pp. 772–776.
- [20] P. Kolodzy “Dynamic Spectrum Policies: Promises and Challenges”, *CommLaw Conspectus*, 2004.
- [21] T. Clancy, “Formalizing the interference temperature model”, *Wiley Journal on Wireless Communications and Mobile Computing*, 7 (9): 1077-1086, 2007.
- [22] J. Bater; H. Tan; K.N. Brown; L. Doyle, “Modelling Interference Temperature Constraints for Spectrum Access in Cognitive Radio Networks,” *IEEE International Conference on Communications (ICC 2007)*, pp. 6493-6498, 24-28 June 2007.
- [23] M. Sharma; A. Sahoo; K.D. Nayak, “Channel modeling based on interference temperature in underlay cognitive wireless networks,” *IEEE International Symposium on Wireless Communication Systems (ISWCS 2008)*, pp.224-228, 21-24 Oct. 2008.
- [24] S.D. Barnes; B.T. Maharaj, “Performance of a Hidden Markov channel occupancy model for cognitive radio,” *AFRICON*, 2011, pp.1-6, 13-15 Sept. 2011.
- [25] T. Yucek, H. Arslan, “A survey of spectrum sensing algorithms for cognitive radio applications”, *IEEE Communication Surveys & Tutorials*, 11 (1): 116-130, 2009.
- [26] R.G. Baraniuk, “Compressive Sensing [Lecture Notes],” *Signal Processing Magazine, IEEE*, Vol. 24, No. 4, pp.118-121, July 2007.

- [27] S.S. Chen, D.L. Donoho, M.A. Saunders; “Atomic decomposition by basis pursuit”, *SIAM Journal on Scientific Computing*, 20 (1998), pp. 33-61.
- [28] M.A. Davenport, P.T. Boufounos, M.B. Wakin, R.G. Baraniuk, “Signal Processing With Compressive Measurements,” *IEEE Journal of Selected Topics in Signal Processing*, Vol. 4, No. 2, pp. 445-460, April 2010.
- [29] J.A. Tropp, J.N. Laska, M.F. Duarte, J.K. Romberg, R.G. Baraniuk, “Beyond Nyquist: Efficient Sampling of Sparse Bandlimited Signals,” *IEEE Transactions on Information Theory*, Vol. 56, No. 1, pp. 520-544, Jan. 2010.
- [30] Y.C. Eldar, G. Kutyniok, *Compressed Sensing*, Cambridge University Press, June 2012.
- [31] Q. Zhao, B.M. Sadler, “A survey of dynamic spectrum access: signal processing, networking, and regulatory policy”, *IEEE Signal Processing Mag.*, Vol. 4, No. 3, pp. 79-89, May 2007.
- [32] L. Rabiner, “A tutorial on hidden Markov models and selected applications in speech recognition,” *Proceedings of the IEEE*, Vol. 77, No. 2, pp.257-286, Feb 1989.
- [33] A.P. Dempster, N.M. Laird, D.B. Rubin, “Maximum likelihood from incomplete data via the EM algorithm”, *J. Roy. Stat. Soc.*, Vol. 39, No. 1, pp. 1-38, 1977.
- [34] L.E. Baum, G.R. Sell, “Growth functions for transformations on manifolds”, *Pac. J. Math.*, Vol. 27, No. 2, pp. 211-227, 1968.
- [35] J.K. Baker, “The dragon system-An overview”, *IEEE Trans. Acoust. Speech Signal Processing*, Vol. ASP-23, No. 1, pp. 24-29, Feb. 1975.